CHIN. PHYS. LETT. Vol. 29, No. 1 (2012) 017803

Comparative Study of the Characteristics of the Basal Plane Stacking Faults of Nonpolar *a*-Plane and Semipolar (11$\bar{2}$2) GaN *

XU Sheng-Rui(许晟瑞)**, LIN Zhi-Yu(林志宇), XUE Xiao-Yong(薛晓咏), LIU Zi-Yang(刘子扬), MA Jun-Cai(马俊彩), JIANG Teng(姜腾), MAO Wei(毛维), WANG Dang-Hui(王党会), ZHANG Jin-Cheng(张进成), HAO Yue(郝跃)

Key Lab of Wide Band-Gap Semiconductor Technology, School of Microelectronics, Xidian University, Xi'an 710071

(Received 13 September 2011)

Nonpolar (11$\bar{2}$0) and semipolar (11$\bar{2}$2) GaN are grown on r-plane and m-plane sapphire by MOCVD to investigate the characteristics of basal plane stacking faults (BSFs). Transmission electron microscopy reveals that the density of BSFs for the semipolar (11$\bar{2}$2) and nonpolar a-plane GaN template is 3×10^5 cm^{-1} and 8×10^5 cm^{-1}, respectively. The semipolar (11$\bar{2}$2) GaN shows an arrowhead-like structure, and the nonpolar a-plane GaN has a much smoother morphology with a streak along the c-axis. Both nonpolar (11$\bar{2}$0) and semipolar (11$\bar{2}$2) GaN have very strong BSF luminescence due to the optically active character of the BSFs.

PACS: 78.55.Cr, 81.15.Kk DOI:10.1088/0256-307X/29/1/017803

Fields exist in Ⅲ-nitride quantum well (QW) heterostructures grown on *c*-plane GaN, and can cause significant separation between the electron and hole carrier wave functions and a redshift of the recombination energy.[1−4] The separation of the electron and hole wave functions caused by the field is most pronounced for InGaN/GaN QW structures with high In content.[2] Therefore, there has been considerable interest in the growth of gallium nitride along the nonpolar and semipolar directions, which can delete or reduce the quantum-confined Stark effect, and in turn the carrier recombination rate in InGaN/GaN QWs. Given a very limited supply and the high cost of GaN substrates sliced from hydride vapor phase epitaxy, the heteroepitaxy of nonpolar and semipolar GaN on *r*-plane and *m*-plane sapphire will likely remain crucial to practical commercialization. Previous reports have shown that the dislocation density of $\sim10^{11}$ cm^{-2} and the basal plane stacking faults (BSFs) of $\sim10^5$ cm^{-1} were found in semipolar and nonpolar GaN under different growth conditions, while the former was believed to limit the room-temperature internal quantum efficiency of nonpolar InGaN/GaN structures.[5−7] BSFs induce a built-in electric field along the *c*-axis, causing in-plane carrier separation and junction leakage current.[8] More recently, the phenomenon that quantum-wire-like features formed by BSFs intersecting the QWs provide a highly efficient light emission dominating the optical properties of the structures was reported.[9] However, the origin of the BSFs in nonpolar and semipolar GaN is still not identified. In fact, a comparison of the properties associated with BSFs between nonpolar and semipolar GaN will probably be helpful in finding the intrinsic mechanism of BSFs in GaN from a different view. In this study, the morphological, crystalline and optical characteristics of the nonpolar and semipolar films grown by metal organic chemical vapor deposition (MOCVD) are investigated.

The growth of the *a*-plane GaN films was achieved on *r*-plane (1$\bar{1}$02) sapphire substrates using a cold-wall showerhead MOCVD system. Hydrogen was used as the carrier gas and triethylgallium, trimethylaluminium and ammonia (NH_3) were used as the source compounds. A low-temperature AlN (LT-AlN) nucleation layer, a high-temperature AlN (HT-AlN) layer and a high-temperature AlN/AlGaN with 10 periods were grown at 620, 1050 and 1020℃, respectively. The growth details of the *a*-plane GaN template are reported elsewhere.[3] Then, Ti films with a thickness of 5 nm were deposited on the template surface by e-beam evaporation, and nitrided in an atmosphere of ammonia and hydrogen for 10 min at 1020℃ to form TiN, with the purpose of improving the crystalline quality of the nonpolar GaN film.[4] The growth of the (11$\bar{2}$2) semipolar GaN film was achieved on *m*-plane sapphire substrates using the same MOCVD system. Before growth, *m*-plane sapphire was nitridized during temperature ramping up to 1080℃ in an NH_3 environment to restrain the (10$\bar{1}$3) mixed phases.[6] The as-grown samples were characterized by scanning electron microscopy (SEM), transmission electron microscopy (TEM) and photoluminescence (PL).

TEM samples were prepared by mechanical polishing before ion-beam thinning to electron transparency in a cross section. The TEM images were acquired on a Tecnai G2 F20 S-Twin operating at 300 kV. Generally, most of the observed BSFs were of I_1 type, nor-

*Supported by the Fundamental Research Funds for the Central Universities under Grant No K50511250002, the National Key Science & Technology Special Project under Grant No 2008ZX01002-002, the Major Program and State Key Program of the National Natural Science Foundation of China under Grant Nos 60890191 and 60736033.

**Correspondence author. Email: shengruixidian@126.com

© 2012 Chinese Physical Society and IOP Publishing Ltd

mally bounded by Frank–Shockley partial dislocations (PDs) ($\boldsymbol{b} = \frac{1}{6}\langle 2\bar{2}03\rangle$). There were also some I_2-type BSFs bounded by Shockley PDs ($\boldsymbol{b} = \frac{1}{3}\langle 1\bar{1}00\rangle$), as well as a few PSFs interconnecting the adjacent BSFs.[10] Figure 1(a) shows the TEM images of the semipolar GaN using $\boldsymbol{g} = 1\bar{1}00$, so the BSFs are edge-on and in contrast. The BSFs are all along the a-axis, so the defects are confined to the c-plane. The density of BSFs decreases as the thickness increases, which should be associated with the tilt characteristic of the semipolar GaN. It can be found that both the a- and c-axes have an angle with the growth $(11\bar{2}2)$ plane. Generally, the a- or c-plane is the major growth plane, so the GaN along the a- and c-directions could obtain a smooth surface under the optimized condition, but nearly all the reported semipolar GaN materials have very rough surface morphologies.[11,12] The rough morphology of the semipolar GaN during growth is propitious for stopping the propagation of inclined BSFs at the coalescence boundary. Indeed, the unique feature of the semipolar GaN was successfully used to improve the crystalline quality.[13] In contrast to the semipolar $(11\bar{2}2)$ plane case, the nonpolar a-plane GaN has a very stable BSF density to the surface until the interface of the TiN interlayer. The BSF densities were found to be $3 \times 10^5\,\mathrm{cm}^{-2}$ and $8 \times 10^5\,\mathrm{cm}^{-2}$ for the semipolar and nonpolar GaN templates, though the BSF density of nonpolar GaN reduced to $2 \times 10^5\,\mathrm{cm}^{-2}$ after the effect of the 5 nm TiN interlayer. For the purpose of giving a clear understanding of the semipolar $(11\bar{2}2)$ plane GaN, the crystal structure with c-, m- and a-axes is shown in Fig. 2. The plane marked by the dotted line is the $(11\bar{2}2)$ plane.

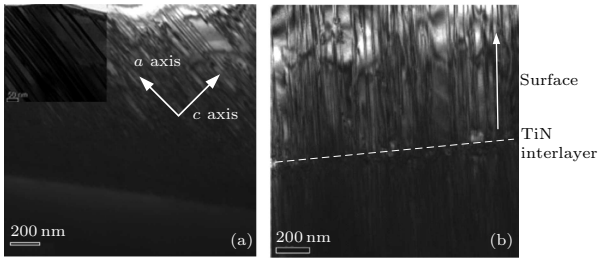

Fig. 1. Cross-sectional TEM images of (a) the semipolar $(11\bar{2}2)$ GaN and (b) the nonpolar a-plane GaN with a 5 nm thick Ti interlayer, using $\boldsymbol{g} = 1\bar{1}00$, with edge-on and in-contrast BSFs.

The standard growth axes (a and c) not only affect the direction of the BSFs, but also play an important role in the morphology of nonpolar and semipolar GaN. Figure 3 shows SEM images of semipolar $(11\bar{2}2)$ GaN on m-sapphire and nonpolar a-plane GaN on r-sapphire. The surface morphology of the semipolar $(11\bar{2}2)$ GaN sample, as shown in Fig. 3(a), has an arrowhead-like structure, which may be caused by the incorporation probability and the diffusion length of the surface atoms toward anisotropic crystallographic directions such as $[\bar{1}\bar{1}23]$ and $[1\bar{1}00]$.[11] Another reason could be that the surface of semipolar $(11\bar{2}2)$ GaN has an angle with respect to the standard growth axis. In contrast, the nonpolar a-plane GaN has a very smooth surface, as shown in Fig. 3(b). Furthermore, a streak-like surface, shown by atomic force microscopy, was reported in our previous work.[3] Both the arrowhead-like and streak-like surfaces can reflect the anisotropy characteristics of the nonpolar a-plane and semipolar $(11\bar{2}2)$ GaN, and the BSFs have been linked to the anisotropic surface morphology.[2]

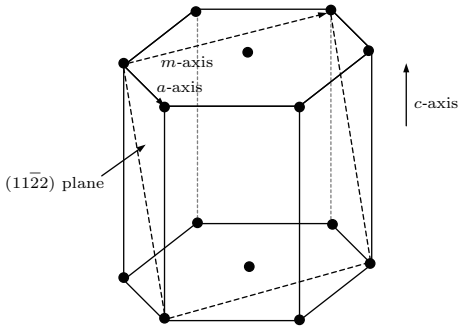

Fig. 2. The relative station of the $(11\bar{2}2)$ plane with a-, c- and m-axes.

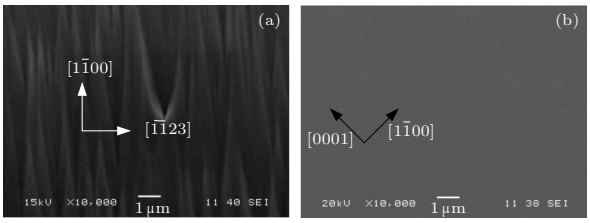

Fig. 3. SEM images of (a) the semipolar $(11\bar{2}2)$ GaN on m-sapphire and (b) the nonpolar a-plane GaN template on r-sapphire.

Moreover, we examined the optical properties of the semipolar $(11\bar{2}2)$ and nonpolar a-plane GaN template. A 325 nm He-Cd laser was used to perform the PL measurement, and the output power of the laser was set constantly to 10 mW at room temperature. The low-temperature PL results measured at 10 K are shown in Fig. 4, where six emission peaks can be found at about 3.48, 3.42, 3.29, 3.04, 2.84 and 2.2 eV, respectively. The 3.47 eV peak is associated with the near band edge (NBE) donor-bound exciton (D^0X), and the 3.42 eV emission has been identified to be involved in BSFs of type-I_1.[14] The density of BSFs is higher than in the conventional c-plane GaN, even in the layers prepared by the traditional lateral epitaxial overgrowth technique. Thus, it can be explained that the 3.42 eV emission band always dominates the low-temperature PL spectra and is much stronger than the NBE emission in nonpolar layers. The emission at 3.29 eV is the effect of PDs terminating the BSFs. The 3.04 eV peak is associated with donor acceptor pair transitions.[15] The 2.84 eV emission is the blue luminescence that exists in many GaN materials, and the 2.2 eV peak is the well-known yellow luminescence

(YL) that is attributed to the transition from shallow donors or the conduction band to deep acceptors.

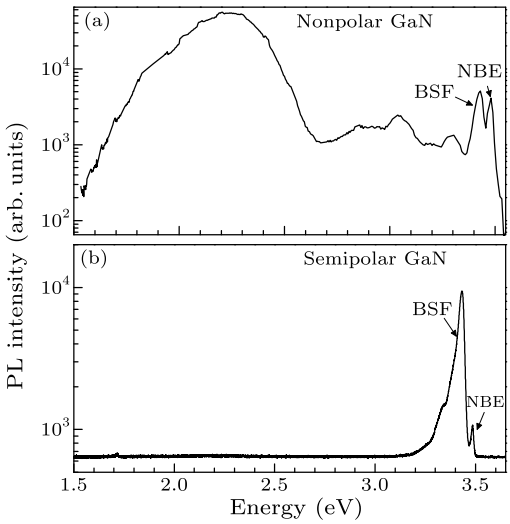

Fig. 4. A typical low-temperature photoluminescence spectrum of our MOCVD grown on (a) a-plane GaN template layers and (b) semipolar $(11\bar{2}2)$ GaN layers.

The emission of the semipolar GaN shows a significant difference with the nonpolar a-plane GaN. The PL spectrum of the semipolar GaN layer, as shown in Fig. 4(b), has an NBE at 3.48 eV assigned to the D^0X, a very strong BSF emission at 3.42 eV and a PD emission at 3.33 eV. The full width at half maximum (FWHM) of NBE for the nonpolar a-plane GaN is 34 meV, but it is only 15 meV for the semipolar $(11\bar{2}2)$ plane GaN. It should be noted that the majority of dislocations are the PDs associated with BSFs in nonpolar and semipolar GaN. The high defect density of PDs is believed to limit the efficiency of radiative recombination. Thus it is unsurprising that the semipolar $(11\bar{2}2)$ plane GaN shows a much smaller FWHM of NBE than the nonpolar a-plane GaN template. Generally, TDs are known to act as nonradiative recombination centers, but BSFs are optically active since they can be considered as cubic (zincblende) ABC phases in the wurtzite ABAB stacking sequence in GaN film. Such a structure forms a type-II heterojunction which could capture electrons and holes, resulting in optical transitions below the wurtzite GaN bandgap energy.[9,16] Therefore, the phenomenon that the PL spectrum shows a very strong BSF luminescence can be explained. In addition, there is still another significant difference between the nonpolar $(11\bar{2}0)$ and semipolar $(11\bar{2}2)$ GaN template: the YL of the semipolar $(11\bar{2}2)$ GaN is very weak, but the YL in the nonpolar a-plane GaN is very strong. The origin responsible for the YL in GaN and the different characteristics of YL are reported elsewhere.[17] The low YL of the semipolar $(11\bar{2}2)$ GaN should be an advantage for application in light-emitting diodes (LEDs).

In summary, we grew nonpolar $(11\bar{2}0)$ and semipolar $(11\bar{2}2)$ GaN on r-plane and m-plane sapphire by MOCVD, respectively. The BSF densities are found to be 3×10^5 cm^{-1} and 8×10^5 cm^{-1} for the semipolar $(11\bar{2}2)$ and nonpolar a-plane GaN templates by the TEM test, and the BSFs of semipolar GaN show a tilt characteristic that should be associated with the crystal structure. The surface structure of the semipolar $(11\bar{2}2)$ GaN sample has arrowhead-like structures that should be affected by the BSFs. Due to the fact that the BSFs are optically active, both the semipolar and nonpolar GaN show a strong BSF luminescence. The FWHM of NBE for the nonpolar a-plane GaN is 34 meV, which is much larger than the 15 meV of the semipolar $(11\bar{2}2)$ plane GaN. The low YL characteristic of the semipolar $(11\bar{2}2)$ plane GaN should be an advantage for application in LEDs.

References

[1] Waltereit P, Brandt O, Trampert A, Grahn H T, Menniger J, Ramsteiner M, Reiche M and Ploog K H 2000 *Nature* **406** 865
[2] Xie Z L, Zhang R, Han P, Zhou S M, Liu B, Xiu X Q, Chen P, Shi Y, Zheng Y D 2008 *Chin. Phys. Lett.* **25** 2614
[3] Xu S R, Hao Y, Zhang J C, Zhou X W, Yang L A, Zhang J F, Duan H T, Li Z M, Wei M, Hu S G, Cao Y R, Zhu Q W, Xu Z H and Gu W P 2009 *J. Cryst. Growth* **311** 3622
[4] Xu S R, Zhang J C, Yang L A, Zhou X W, Cao Y R, Zhang J F, Xue J S, Liu Z Y, Ma J C, Bao F and Hao Y 2011 *J. Cryst. Growth* **32** 94
[5] Moram M A, Johnston C F, Kappers M J and Humphreys C J 2009 *J. Cryst. Growth* **311** 3239
[6] Xu S R, Hao Y, Yang L A, Zhang J C, Xue J S, Xue X Y, Liu Z Y, Lin Z Y, Ma J C, Li P X, Li J T and He Q 2011 *Jpn. J. Appl. Phys.* **50** 115502
[7] Schubert M F, Chhajed S, Kim J K, Fredschubert E, Koleske D D, Crawford M H, Lee S R, Fischer A J, Thaler G and Banas M A 2007 *Appl. Phys. Lett.* **91** 231114
[8] Chakraborty A, Haskell B A, Keller S, Speck J S, Denbaars S P, Nakamura S and Mishra U K 2005 *Jpn. J. Appl. Phys.* **44** L173
[9] Jönen H, Rossow U, Bremers H, Hoffmann L, Brendel M, Dräger A D, Schwaiger S, Scholz F, Thalmair J, Zweck J and Hangleiter A 2011 *Appl. Phys. Lett.* **99** 011901
[10] Sun Q, Kong B H, Yerino C D, Ko T S, Leung B, Cho H K and Han J 2009 *J. Appl. Phys.* **106** 123519
[11] Oh D S, Jang J J, Nam O, Song K M and Lee S N 2011 *J. Cryst. Growth* **326** 33
[12] Wernicke T, Netzel C, Weyers M and Kneissl M 2008 *Phys. Status Solidi* C **5** 1815
[13] Mierry P D, Kriouche N, Nemoz M and Nataf G 2009 *Appl. Phys. Lett.* **94** 191903
[14] Paskov P P, Schifano R, Monemar B, Paskova T, Figge S and Hommel D 2005 *J. Appl. Phys.* **98** 093519
[15] Netzel C, Wernicke T, Zeimer U, Brunner F, Weyers M and Kneissl M 2008 *J. Cryst. Growth* **310** 8
[16] Stampfl C and VandeWalle C G 1998 *Phys. Rev.* B **57** 15052
[17] Xu S R, Hao Y, Zhang J C, Cao Y R, Zhou X W, Yang L A, Ou X X, Chen K and Mao W 2010 *J. Cryst. Growth* **312** 3521